Int J Thermophys (2008) 29:1668–1677
DOI 10.1007/s10765-008-0457-2

Investigation of Capacitive-Based Relative Humidity Sensors and Their Stability at High Temperature

V. Fernicola · M. Banfo · L. Rosso · D. Smorgon

Published online: 11 June 2008

Abstract The performance of high-temperature, polymer-based RH sensors was investigated in order to evaluate their long-term stability. The work is aimed at understanding how severe temperature cycles may alter the characteristics of relative humidity (RH) sensors, how they impact the measurements, and how they contribute to the measurement uncertainty. The tests involved 10 high-temperature RH sensor probes available from five European manufacturers. They were initially calibrated against suitable humidity standards in the range from 10 %rh to 85 %rh with air temperatures from 20 °C to 80 °C, and subsequently, they were exposed to air temperature at about 145 °C for several cycles, each cycle lasting (50–100) h. After each high-temperature exposure, a calibration check at 80 °C was carried out. The test lasted until the sensor exposure time exceeded 300 h. The paper presents the characteristics of such probes, the investigation results, and the comparison of the specified versus the experimental performances.

Keywords High-temperature testing · Humidity · Polymeric sensors · Relative humidity · Sensor stability

1 Introduction

Relative humidity (RH) sensors are finding widespread use in both traditional and emerging applications. Air conditioning, energy saving, and domotics require RH sensors with a comparatively narrow temperature working range, while industrial process control and the automotive industry need reliable RH sensors with a broad operating

V. Fernicola (✉) · M. Banfo · L. Rosso · D. Smorgon
Thermodynamics Division, Istituto Nazionale di Ricerca Metrologica (INRIM), Strada delle Cacce 91, 10135 Torino, Italy
e-mail: v.fernicola@inrim.it

temperature range and improved stability. In many cases, it happens that the sensor used for measurements in a moderate temperature range (e.g., 0 °C to 80 °C) can also be exposed to higher environmental temperatures. This is the case, for example, of the control probes used in climatic enclosures and chambers for environmental testing of electronic components and devices and for THB (temperature humidity bias test) and HAST (highly accelerated stress test) testing. Such probes are often used to control RH when the air temperature is below 100 °C; for higher temperatures, such as during thermal aging and qualification tests, the RH control is not in operation but the system temperature could cycle up to 150 °C and above. The sensing probe of such control systems was generally a psychrometer; nowadays, it is often replaced by a low-cost, polymeric, capacitive-based sensor. Polymer-based RH sensors are also used as the reference probe in portable humidity generators and other precision measurement applications. Several reports can be found in the technical and scientific literature about their metrological characteristics. Long-term stability studies of polymeric sensors at ambient temperature were reported [1]; performance limitations and calibration errors due to temperature immersion effects up to 30 °C and 90 %rh were also investigated [2,3]. The temperature dependence of the calibration curve was also discussed by other authors [4]. The results showed that, despite a significant improvement in sensor technology and manufacturing capability over the years, a large variability of temperature sensitivities can still be found in industrial sensors [5].

The present work is aimed at investigating the characteristics of high-temperature RH sensors and how their long-term stability is affected by the temperature when they are exposed to air temperatures above 100 °C. The main goal of the study is to understand the performance and limitations of the polymeric-type sensors; consequently, the results are presented in an anonymous form in order to avoid any commercial comparison among the selected systems.

2 Experimental Details

2.1 Sensor Specifications and Characteristics

A capacitive-based humidity sensor relies on a change in the dielectric properties of a thin polymer film upon interaction with water-vapor molecules. The resulting permittivity change of the device can thus be measured by standard capacitive sensing methods. Industrial systems are generally made of two parts: a measuring probe, with or without some signal conversion features, and a data transmission unit.

Ten high-temperature probes available from commercial off-the-shelf production from five European manufactures were selected for the tests [6–10]. They are novel devices, with improved performance and a broader temperature range, and they are deemed representative of the instrumentation currently used in many industrial measurement and testing applications.

The main specifications of the sensors, as available from manufacturer data sheets, are summarized in Table 1. The measuring probe body was made of either stainless steel or a high-temperature polymer. The transmitter output can be either a DC analog current or a DC analog voltage signal. Two identical sensor probes from each

Table 1 Technical specifications of the capacitive RH sensors under test as available from the manufacturers' datasheets

Manufacturers	Delta Ohm	E+E	Rotronic	Testo	Vaisala
Model	HD2008TC/2	EE31 PFTD	HygroFlex HTS1 (IC-3)	HygroTest 650 PHT	HMT 325 HMP305
RH measurement range (%rh)	5–98	0–100	0–100	0–100	0–100
T measurement range (°C)	−40 to +150	−40 to +180	−50 to +200	−20 to +180	−40 to +180
Accuracy (%rh)					
(0–100)			±1[f]	±2	
(0–90)	±2[f]	±2[c]			±1[a]
(90–100)	±2, 5[f]	±3[c]			±2[a]
Temp. Coefficient (%rh · °C^{-1})		±0.01[d,e]		±0.05[b]	
Long-term stability (%rh)			<1		
Analog output	(4–20) mA	(4–20) mA	(4–20) mA	(4–20) mA	(0–1) V
Stem size (o.d.—length, mm)	12.5–330	12–215	11–265	12–221	12–225
Stem body	Polymeric	Stainless steel	Stainless steel	Stainless steel	Stainless steel

[a] Accuracy includes sensor temperature dependence, nonlinearity, hysteresis, and repeatability.
[b] At temperatures different from 25 °C
[c] Accuracy includes hysteresis and nonlinearity
[d] Temperature dependence of electronics
[e] Temperature dependence of sensing probe: ± (0.002 + 0.0002 · reading/%rh) · (T/°C—20)
[f] Uncertainty at ambient temperature

manufacturer were selected in order to investigate probe-to-probe variability. In the reported measurements, the devices were identified as A1–A2 to E1–E2 (i.e., same letter and consecutive number for probes coming from the same manufacturer).

2.2 Measurement System and Procedure

The investigations of the RH sensors were carried out using two different measurement setups. Initial and final calibrations were performed against the INRIM two-temperature humidity standard generator [11]. The probes were inserted into the test chamber of the generator where the reference RH was generated by means of gas-tight adapters that matched the test chamber port size and the outer diameter of each stem. The calibrations were carried out at 25 °C and 80 °C air temperature with the probe stem partially immersed (about 100 mm) into the chamber. The total immersion depth of the probes into the temperature bath housing the generator test chamber was about 180 mm. With this setup, the immersion error due to conduction along the probe stem was greatly reduced [2]. Three intermediate calibrations (steps 2–4) at 80 °C were carried out in a climatic chamber by comparison against a calibrated chilled-mirror hygrometer and a PRT air-temperature probe whose readings were used to calculate the reference RH [12,13]. A 6 ½ digit DVM-based data acquisition system was used to collect the signal output from the transmitter associated with each sensor.

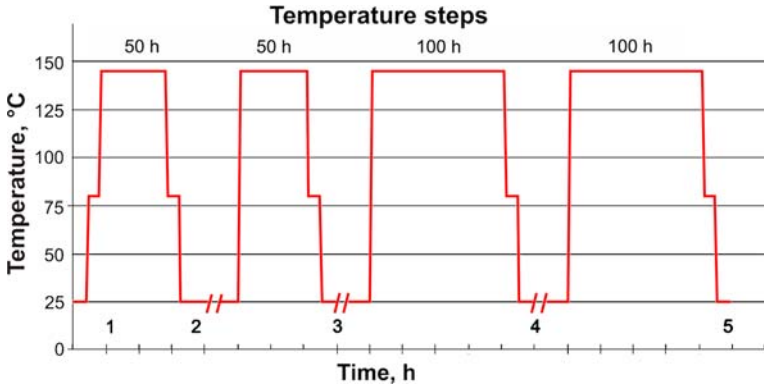

Fig. 1 Overview of the experimental procedure: the calibration at steps 1 and 5 was carried out at 25 °C and 80 °C; at the intermediate steps (2–4), a high-temperature exposure at 145 °C was followed by a calibration at 80 °C

Calibrated, low-TC, metal-film resistances were used to convert the DC current output (4–20 mA) from each transmitter.

Figure 1 shows a schematic of the experimental procedure and measurement steps. Step 1 and step 5 concern the initial and final calibrations. The calibration at 25 °C was carried out at increasing humidity (25 %rh to 80 %rh); a repeat point at 50 %rh was also performed at decreasing humidity. The calibration at 80 °C was carried out at increasing humidity (10 %rh to 80 %rh); a repeat point at 50 %rh was performed at decreasing humidity.

Before any further calibrations at 80 °C, the sensor probes were inserted in a thermowell of a temperature-controlled furnace and were exposed to air temperature at about 145 °C. The repeated high-temperature soaking lasted (50–100) h each, with a total thermal exposure of about 300 h. After each calibration at 80 °C, and before any new high-temperature exposure, the probes were stored in the laboratory at ambient temperature for several weeks.

2.3 Calibration Uncertainty

The uncertainties of the RH sensor calibration were calculated from the input standard uncertainties grouped into three main categories [14]:

- uncertainty of the reference conditions, provided either by the humidity standard generator in the test chamber [11] or by a calibrated chilled-mirror hygrometer and a PRT air temperature in the climatic chamber [13];
- uncertainty arising during the measurement process, including the fluctuation in the physical conditions of the test;
- uncertainty of the device under calibration, including contributions from the resolution, and repeatability of the reading.

From the RH ϕ expressed in decimal form:

$$\phi = \frac{f(t_d, p)\, p_{vs}(t_R)}{f(t_a, p)\, p_{vs}(t_a)} \approx \frac{p_{vs}(t_d)}{p_{vs}(t_a)} \tag{1}$$

and from the uncertainty propagation law, the combined standard uncertainty is:

$$u^2(\phi) = \left\{ \left[\frac{\partial \phi}{\partial t} \right]^2_{t=t_\mathrm{d}} u^2(t_\mathrm{d}) + \left[\frac{\partial \phi}{\partial t} \right]^2_{t=t_\mathrm{a}} u^2(t_\mathrm{a}) \right\} = \alpha_1^2(t_\mathrm{d}) u^2(t_\mathrm{d}) + \alpha_2^2(t_\mathrm{a}) u^2(t_\mathrm{a}) \quad (2)$$

where $\alpha_1(t_d)^2$ and $\alpha_2(t_a)^2$ are the sensitivity coefficients with respect to the dew point and air temperature, respectively. The RH standard uncertainty is thus obtained from

$$u(RH) = 100 \times \sqrt{u^2(\phi)} \quad (3)$$

In the measurement range of interest for this work, i.e., from 10 %rh to 80 %rh with air temperature from 20 °C to 80 °C in the test chamber of the standard generator, a calibration uncertainty of (0.29–0.45) %rh resulted, while in the climatic chamber a calibration uncertainty of (0.61–1.15) %rh resulted.

3 Results

3.1 Comparison Between Initial and Final Calibrations

3.1.1 Drift

Figure 2a–e shows initial (step 1) and final (step 5) calibrations at 25 °C for all the sensors. Each graph shows the calibration correction (i.e., reference RH minus RH reading) for two sensor probes of the same manufacturer. The analysis of the initial and final calibration data at 25 °C showed that 8 sensors out of 10 had a considerable drift; for some sensors (A and E), the readings were up to 3 % higher at the end of the test. Figure 2 shows that the results were quite repeatable between probes of the same manufacturer, i.e., all the probe pairs, except those from manufacturer D, presented quite homogeneous behavior. The sensors that showed the best performance in this test were B1 and B2, which drifted less than 1.5 %rh. They also show the best probe-to-probe repeatability, both at the beginning and at the end of the test.

3.1.2 Hysteresis

Hysteresis can significantly contribute to the measurement uncertainty, but it is not always specified by the manufacturers. Figures 2a–e and 3 show how the sensor hysteresis significantly changed during the tests for all sensors, except for those from manufacturer C, which remained fairly constant from the beginning to the end of the test. In one case, sensor D1, the hysteresis was smaller at the final than at the initial calibration; however, such behavior was not reproduced by sensor D2. Initial hysteresis was within 1 % for sensors A, B, and E and around 2 % for sensors C and D. Final hysteresis was still found to be within 1 % for sensor B, but with an unexpected sign change; it increased significantly (up to 4 % and above) for sensors A, D, and E.

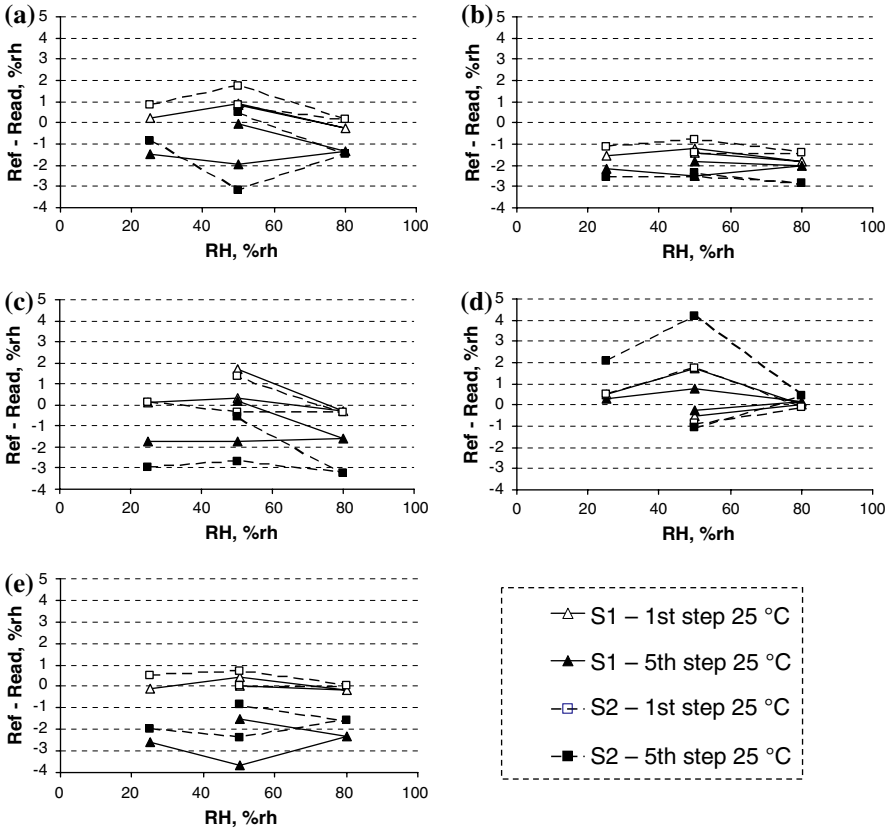

Fig. 2 Calibration correction curves (i.e., reference value minus sensor reading) at 25 °C air temperature for selected sensors, as obtained at the initial (1st step) and final (5th step) calibration

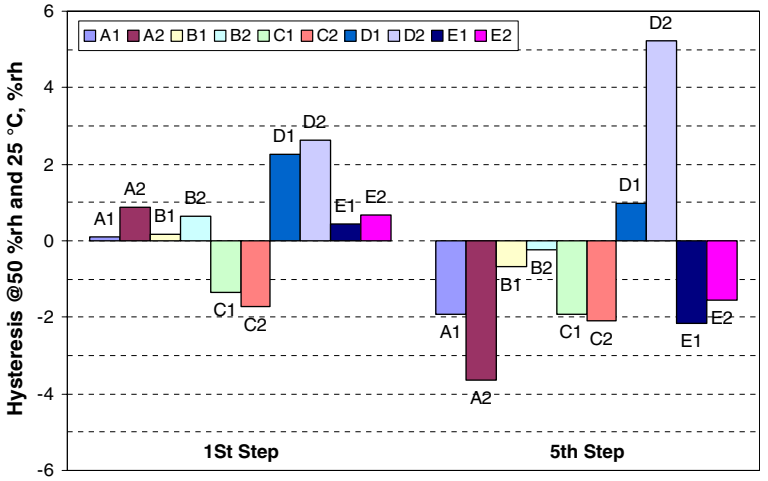

Fig. 3 Summary of the sensor hysteresis at 50 %rh after the first and last calibrations at 25 °C air temperature

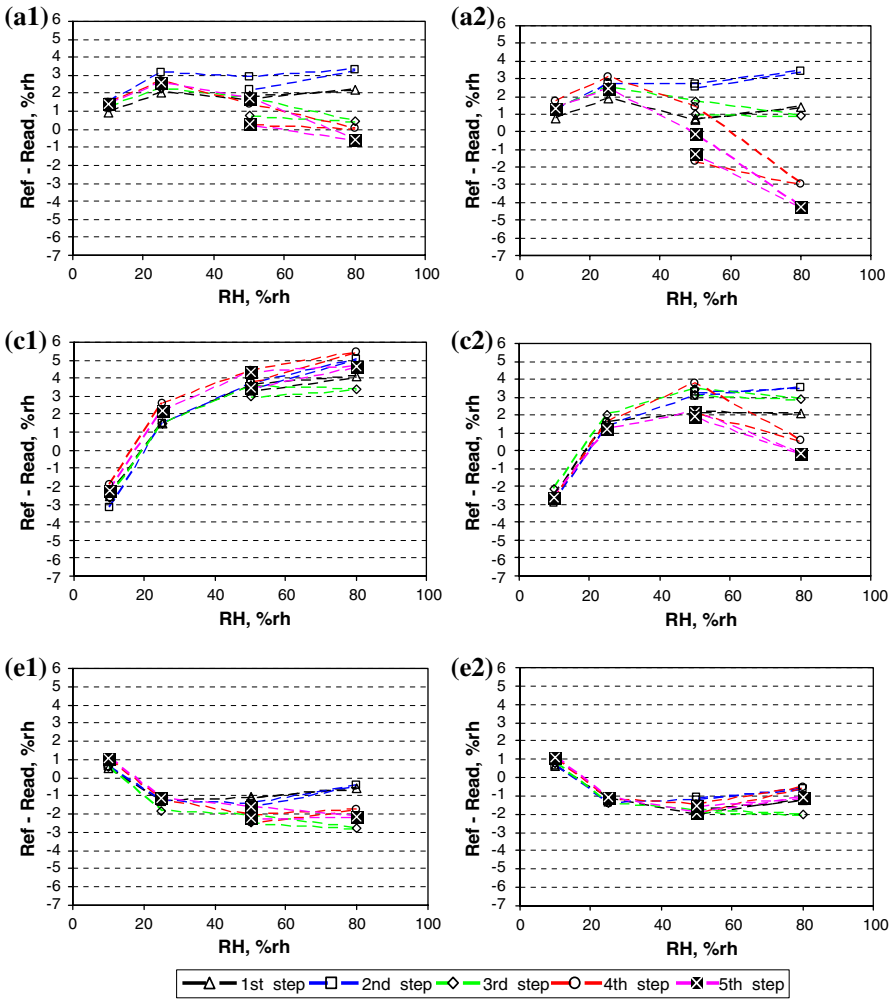

Fig. 4 Calibration correction curves and drift at 80 °C air temperature, after each intermediate high-temperature exposure at 145 °C (2nd to 4th steps)

3.2 Intermediate Calibrations at 80 °C

The main purpose of this set of tests is to investigate how thermal aging affected the sensors' performance and how they responded to repeated soakings in a high-temperature environment. Figure 4 summarizes the most significant calibration results at 80 °C for selected groups of sensors (A, C, and E). The graphs are laid out as follows: sensors of the same manufacturer, tested in separate runs, share a horizontal row; sensors of different manufacturer, tested in the same run, share the same column.

Samples of the same family, such as sensor pair A1–A2, showed a different behavior with respect to thermal drift over time; e.g., for sensor A2 the calibration correction

at 80 %rh greatly changed during the course of the tests, i.e., from about +3 % to −4 %, while this was not the case for sensor A1. Sensor pairs C1–C2 and E1–E2 showed quite homogeneous and stable behavior during the calibration runs carried out after each high-temperature exposure. It should be noted, however, that sensors C1–C2 showed a large nonlinearity with a calibration correction spanning over 8 %rh in the range. On the contrary, the linearity and the stability of the calibration curves of sensors E1–E2 were remarkably good. The sensors had almost no tendency to drift, even after 300 h at 145 °C.

3.3 Temperature Sensitivity

The temperature sensitivity of an RH probe would generally result from several temperature-dependent effects arising from the sensor and the associated electronics. All probes are configured with their signal processing and transmitter unit physically separated from the sensor probe. In this case, only the sensing element was exposed to temperature cycles, while the electronics always operated at ambient temperature.

Each graph in Fig. 5 shows the initial and final temperature coefficients (TCs) for some selected sensors, as detected at three relative-humidity values (i.e., 25 %rh, 50 %rh, and 80 %rh). They were calculated from the calibration curves at 25 °C and 80 °C. A straight-line fit to the points shows the average TC slope. The graphs that share a row refer to the initial and final temperature sensitivities of sensors from the same manufacturer; graphs along a column compare the sensors from different manufacturers. Absolute TCs in the range (0.03–0.12) $\%\mathrm{rh}\cdot{}^{\circ}\mathrm{C}^{-1}$ were found. It is interesting to note that sensors from the same manufacturer may have different TCs (i.e., lines are not parallel), and for some of them, the TC changed its sign after the final calibration. A further analysis was carried out in Fig. 6, where the TCs at high humidity (80 %rh) are shown after the initial and final calibration steps. Sensors A, D, and E had the lower absolute TC (below $0.05\,\%\mathrm{rh}\cdot{}^{\circ}\mathrm{C}^{-1}$); however, among them, only sensor D did not change the TC sign from the first to the last calibration. In general, sensors D and E had the least sensitivity to temperature. It should be noted (see Table 1) that only two manufacturers provided technical data for the TC. Unfortunately, in both cases, the manufacturer specifications were not met.

4 Discussion and Conclusions

Polymer-based capacitive sensors are probably the most widespread sensor for RH measurements. They are often used in a wide range of environmental and industrial applications where harsh operating conditions are likely to be met. New polymer materials with improved performance were developed to cope with these measurement challenges, but despite major improvement in high-temperature RH sensor technology and promising technical specifications, this work demonstrated that the sensor may suffer from significant long-term instability when used in extreme conditions.

From the literature and previous work, it is known that such sensors may respond in different ways to varying operating conditions, but unfortunately the manufacturers' specifications do not always offer the whole range of information needed by the user.

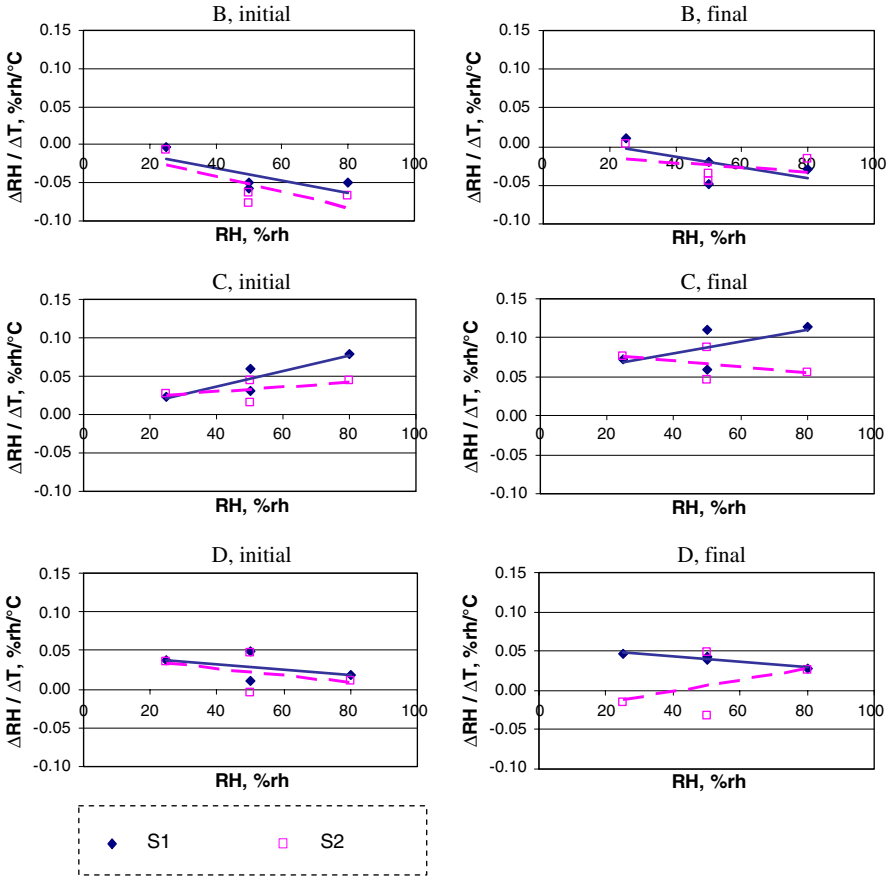

Fig. 5 Temperature sensitivity coefficients $\Delta RH/\Delta T$ (%rh $\cdot\,^{\circ}\mathrm{C}^{-1}$) for selected sensors as a function of the sensor reading after the initial and final calibrations

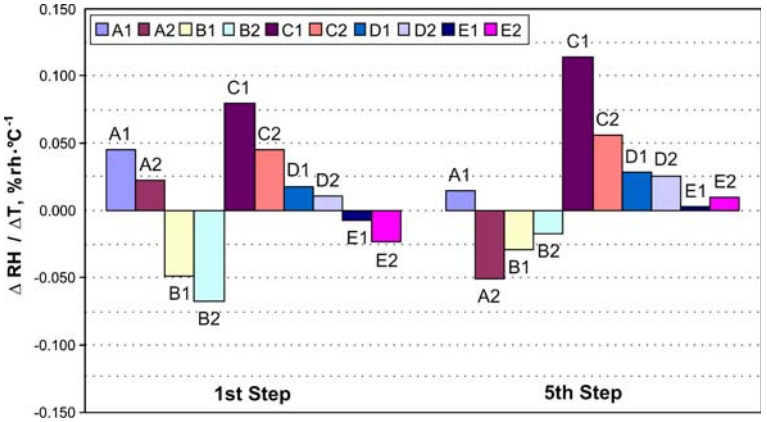

Fig. 6 Summary of the temperature sensitivity coefficients $\Delta RH/\Delta T$ (%rh $\cdot\,^{\circ}\mathrm{C}^{-1}$) at 80 %rh for all sensors after the initial (1st step) and final (5th step) calibrations

On the other hand, a single calibration, even if it could encompass a wide range of temperature and humidity, only shows the performance of the sensor at a given time, while long-term tests are necessary to obtain additional information about the sensor characteristics to determine to what degree it is suited to a specific application.

The work investigated the performance and limitations of such polymeric-type high-temperature RH sensors and how their long-term stability was affected by repeated exposure to air temperature above 100 °C. Ten sensors from five European manufacturers were tested for about a year using the humidity calibration facility available at the INRIM. A large variability among the sensors in terms of linearity, hysteresis, and stability of the calibration curve resulted. While many sensors showed an initial response curve at 25 °C within the tolerances stated by the manufacturers, it was found that the calibration correction at 80 °C can greatly exceed the above tolerances, with sensors exhibiting significant nonlinearity and bias with respect to the reference values. It was also found that the drift, which was mainly triggered by the temperature exposure, was not monotonic with the exposure time and was not uniform throughout the sensors. The tests showed, besides the stability issue, that the effects of hysteresis and the slope of the temperature sensitivity curve must be carefully evaluated, especially for measurements at high RH.

The results led to the conclusion that the traceability of humidity measurements can be difficult to achieve with a high degree of confidence in severe industrial applications. It would also suggest to sensor manufacturers that more efforts are needed to specify sensor performance in order to give sufficient information to the final user.

Acknowledgments The authors kindly acknowledge all companies and manufacturers who made available their humidity sensors to carry out this work.

References

1. G.J.W. Visscher, J.G. Kornet, Meas. Sci. Technol. **5**, 1294 (1994)
2. J. Lovell-Smith, R. Benyon, R. Mason, in *Proceedings of 4th International Symposium on Humidity and Moisture* (CMS, ITRI, Taipei, Taiwan, 2002), pp. 389–396
3. D. Jonker, R. Mokhutshoane, H. Liedberg, in *Proceedings of 4th International Symposium on Humidity and Moisture* (CMS, ITRI, Taipei, Taiwan, 2002), pp. 576–582
4. G. Buonanno, M. Dell'isola, V.C. Fernicola, A. Frattolillo, in *Proceedings of 4th International Symposium on Humidity and Moisture* (CMS, ITRI, Taipei, Taiwan, 2002), pp. 350–358
5. Z.M. Rittersma, Sensor Actuat A: Phys **96**, 196 (2002)
6. Delta Ohm, Mod. HD2008TC/2, http://www.deltaohm.com
7. E+E, Mod. EE31 PFTD, http://www.epluse.at
8. Rotronic, Mod. HYGROFLEX HTS1 (IC-3), http://www.rotronic.com
9. Testo, Md. HYGROTEST 650 PHT, http://www.testo.com
10. Vaisala, Mod. HMT 325 - HMP305, http://www.vaisala.com
11. A. Actis, M. Banfo, V.C. Fernicola, R. Galleano, S. Merlo, in *Proceedings 3rd International Symposium on Humidity and Moisture*, vol. 1 (NPL, Teddington, UK, 1998), pp. 2–9
12. V. Fernicola, M. Banfo, in *Proceedings of TEMPMEKO 2001, 8th International Symposium. on Temperature and Thermal Measurements in Industry and Science*, vol. 2, ed. by B. Fellmuth, J. Seidel, G. Scholz (VDE/Verlag, Berlin, Germany, 2002), pp. 751–756
13. A. Actis, V.C. Fernicola, in *Proceedings of 15th World Congress of the International Measurement Confederation*, vol. VII (Osaka, Japan, 1999), pp. 191–196
14. M. Heinonen, Uncertainty in humidity measurements, EUROMET Workshop P758, *MIKES Publ. J4/2006* (Espoo, Finland, 2006)